Thermal conductivity of carbon nanoring linked graphene sheets: A molecular dynamics investigation*

Gang Shi(石刚), Jianwei Zhang(张鉴炜)†, Yonglv He(贺雍律), Su Ju(鞠苏), and Dazhi Jiang(江大志)‡

Department of Materials Science and Engineering, National University of Defense Technology, Changsha 410073, *China*

(Received 22 June 2017; revised manuscript received 20 July 2017; published online 10 September 2017)

Improving the thermal conduction across graphene sheets is of great importance for their applications in thermal management. In this paper, thermal transport across a hybrid structure formed by two graphene nanoribbons and carbon nanorings (CNRs) was investigated by molecular dynamics simulations. The effects of linker diameter, number, and height on thermal conductivity of the CNRs–graphene hybrid structures were studied respectively, and the CNRs were found effective in transmitting the phonon modes of GNRs. The hybrid structure with 2 linkers showed the highest thermal conductivity of 68.8 $W{\cdot}m^{-1}{\cdot}K^{-1}$. Our work presents important insight into fundamental principles governing the thermal conduction across CNR junctions and provides useful guideline for designing CNR–graphene structure with superior thermal conductivity.

Keywords: carbon nanorins–graphene hybrid structures, thermal conductivity, molecular dynamics simulation

PACS: 65.80.–g, 65.80.Ck, 63.22.–m, 31.15.xv **DOI:** 10.1088/1674-1056/26/10/106502

1. Introduction

With persistent miniaturization of electronic devices, increasing power dissipation density has become an urgent problem to be solved. Due to its ultrahigh in-plane thermal conductivity,[1] graphene has attracted considerable attention in fabrication of high-performance thermal management nanoelectronics.[2–4]

In general, thermal transport in graphene-based devices is limited by the poor thermal conduction between graphene sheets. For example, the thermal conductivity of graphene films consisting of randomly networked graphene sheets is much lower than that of a single graphene sheet.[5] The main reason for this dramatic shortfall lies in the high thermal resistance between adjacent graphene sheets due to weak inter-sheet interactions. For an individual monolayer graphene sheet, the in-plane covalent sp^2 bonds between carbon atoms are among the strongest in nature. By contrast, the interaction between adjacent graphene sheets with spacing of 3.35 Å is mainly governed by weak van der Waals force. As a result, the in-plane thermal conductivity of graphene sheet is superb ($\sim$5300 $W{\cdot}m^{-1}{\cdot}K^{-1}$ [6]), while the out-of-plane thermal conductivity between graphene sheets is rather poor ($<$ 50 $W{\cdot}m^{-1}{\cdot}K^{-1}$ [7]), which has become the limiting factor for the thermal transport of graphene films.[8]

Currently, there is a growing interest in developing three-dimensional (3D) graphene-based nano-devices assembled by graphene sheets and carbon nanotubes (CNTs).[9–11] The CNTs were embedded between graphene sheets, lying parallel to the graphene sheets or acting as pillars to bridge the graphene sheets, which would highly enlarge the inter-sheet spacing.[12] These 3D CNT–graphene structures were with large surface areas and good electrical conductivities, showing potential in high-performance capacitances,[13] hydrogen storage devices,[14] and gas separation membranes.[15] However, in these attempts, the CNTs were with lengths ranging from tens of nanometers to tens of microns, and could not effectively bridge the graphene sheets in a graphene films. So CNTs in these structures could not act as effective heat transport tunnels to enhance the out-of-plane thermal transport between graphene sheets. These structures reported still limited by the low out-of-plane thermal conductivity.

To achieve higher thermal conductivity between graphene sheets, two issues should be addressed. One is that the CNTs should be short enough so as to minimize the inter-sheet spacing effect. The other is that the CNTs should be covalently bonded with the graphene sheets to realize phonon transfer. Sun *et al.*[16] prepared super-short CNTs, namely Carbon nanorings (CNRs), in confined space of two-dimensional interlayer galleries of layered double hydroxide hosts. Their work indicated that the CNRs with height less than one nanometer could be obtained by limiting the confined space. In our previous work, we fabricated a 3D CNR–graphene hy-

*Project supported by the National Natural Science Foundation of China (Grant No. 11202231) and the Research Project of National University of Defense Technology (Grant No. JC15-01-03).

†Corresponding author. E-mail: jwzhang.nudt@gmail.com

‡Corresponding author. E-mail: jiangdz@nudt.edu.cn

© 2017 Chinese Physical Society and IOP Publishing Ltd

brid paper through in-situ growth of CNRs in the inter-gallery space between graphene sheets.[17] This structure possesses outstanding through-plane thermal conductivities, and can be easily integrated into high-power electronics and stretchable devices as multi-functional thermal management materials.

Although some progress has been made, there is still lack of in-depth understanding of the effects of CNR linkers on the thermal transport across the graphene sheets. In order to design a novel pure carbon-based structure with superior thermal properties, e.g., CNR–graphene hybrid structure (CGHS), further understanding of fundamental principles that govern the involved thermal transport is vitally important. Thus, several fundamental but crucial questions need to be deliberated: (i) How do the diameters of CNR linkers affect phonons transferring across CGHS? (ii) How do the linker number influence the thermal resistance across graphene sheets? And (iii) how do the heights of CNRs impact on the thermal conductivity of CGHS?

Given that the current experimental methods are incapable of effectively characterizing the thermal transport between graphene sheets at atomic scale, atomistic simulations provide a powerful and effective tool to illustrate this issue. In this paper, non-equilibrium molecular dynamics (NEMD)[18] simulations were performed to address the questions mentioned above, aiming to provide new insights into the fundamental principles governing the thermal transport across hybrid nano-carbon structures and useful design guidelines for heat management in nano-scaled graphene-based devices.

2. Model and methodology

All models simulating CGHS were built using Materials Studio (Accelrys Inc). For selecting the potential models very important for MD simulations, a COMPASS (Condensed-phase Optimized Molecular Potentials for Atomic Simulations Studies) force-field is applied to describe the inter-atomic chemical bonds and non-bonding potential energy.[19–21] To construct the CGHS, two parallel graphene sheets were constructed in a periodic boundary condition. Circular holes were created on the graphene sheets and an armchair CNR was placed vertically over the pore with the tube ends bonded to two adjacent graphene sheets. The diameter of the pores is the same as that of CNRs. A 30-Å thick vacuum slab along the z-axis direction was built to prevent any interaction between the periodic graphene sheets. Figure 1(a) shows the top view of a CGHS with one CNR linker. The CNR is oriented along z axis. In all simulated cases, geometries of the graphene and their overlapping areas were fixed (Figs. 1(a)–1(c)), that is, the overlap length, $\Delta L = 4.5$ nm, length of graphene sheet one, $L_1 = 17$ nm, length of graphene sheet two, $L_2 = 16.5$ nm, the total length of the CGHS, $L = L_1 + L_2 - 2\Delta L = 24.5$ nm (along the x-axis direction) and the width of the graphene sheets (along the y-axis direction), $W = 4.26$ nm. Meanwhile, the effects of important geometric parameters applied in the simulation were studied by varying diameters and heights of CNRs, linker numbers and linker arrangement. A zoomed-in image of the CNR–graphene junction is shown in Fig. 1(d). Three important regions, namely graphene interfacial region, CNR interfacial region and CNRs bulk region were tagged in Fig. 1(d). These regions are defined because they played an important role in thermal transport across graphene sheets. The centre-to-centre distance between two neighboring CNRs is called the CNR distance (*CD*). The width of graphene sheet minus the diameter of CNR is defined as effective width (*EW*).

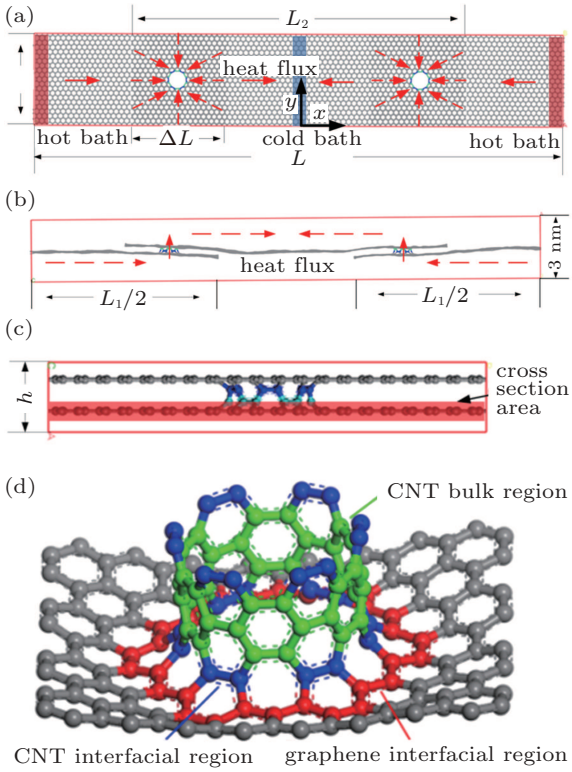


Fig. 1. (color online) Schematic diagram of a CNR–graphene hybrid structure. (a) Top view; (b) Front view; (c) Side view; (d) Schematic diagram of a CNR junction.

The simulation model is energy-minimized to reach equilibration by iteratively adjusting atomic coordinates. The unit cell is partitioned into 50 slabs along the x axis for temperature recording and momentum exchange processes. According to Muller–Plathe algorithm, heat sink and source were placed at the center and each end of the cells to generate constant heat flux, as shown in Fig. 1(a). The heat transfer process includes 3 steps: heat conduction in graphene sheet one, thermal transport across CNR–graphene junction, and heat conduction in graphene sheet two.

The NEMD simulation was conducted using micro-canonical ensemble (NVE) for 500 ps with a fixed time step

of 1.0 fs. The velocity exchanging was performed every 100 fs.[22,23]

The transferred heat is calculated by the accumulation of exchanged kinetic energy as:

$$Q = \sum_{\text{swaps}} (E_{\text{h}} - E_{\text{c}}), \tag{1}$$

where E_{c} and E_{h} are kinetic energy of the cold and hot slabs, respectively. The imposed heat flux J is calculated from:

$$J = \frac{Q}{2A\Delta t}, \tag{2}$$

where the cross sectional area normal to the direction of heat flux is $A = \delta \cdot W$, in which, δ is the wall thickness of graphene. Cross sectional area A of monolayer graphene was used to calculate the thermal conductivity, considering the area of the path through which thermal transport occurs. The thickness of the graphene is assumed to be 1.42 Å, which is the generally accepted C–C bond length and has been used in literatures to obtain thermal conductivity of graphene and CNTs.[24–26] Δt is the simulation time. The heat flux J through the structure was imposed following the NEMD simulation method. When the heat flow in the structure reached a steady state, the heat flux and temperature gradient were recorded and averaged.

The thermal conductivity along x axis is calculated on the basis of Fourier's law. Where κ is the thermal conductivity and $\Delta T/\Delta x$ is the temperature gradient.[27,28]

$$\kappa = \frac{J}{\Delta T/\Delta x}. \tag{3}$$

To understand the underlying mechanisms of phonon transport, the phonon density of states (VDOS) has been studied. The VDOS is calculated from the Fourier transform of the velocity autocorrelation function, which can be expressed as follows:[24]

$$P(\omega) = \frac{1}{\sqrt{2\pi}} \int \mathrm{e}^{-\mathrm{i}\omega t} \left(\sum_{j}^{N} v_j(t)\, v_j(0) \right) \mathrm{d}t, \tag{4}$$

where ω is vibrational wavenumber of phonon, $v_j(t)$ is velocity of atom j at time t, N is atomic number, and $v_j(0)$ is velocity of atom j at initial time. To analyze the underlying mechanisms of the effect of cross-linker on graphene interfacial thermal resistance, the VDOS for pristine graphene, graphene interfacial region, CNR interfacial region, and CNRs bulk region were calculated.

To quantitatively determine the overlap of two VDOS spectra, an overlap factor η is defined as:[29]

$$\eta = \frac{\int_0^{+\infty} \min\left[P_1(\omega), P_2(\omega)\right] \mathrm{d}\omega}{\int_0^{+\infty} P_1(\omega)\, \mathrm{d}\omega}, \tag{5}$$

P_1 and P_2 are the normalized VDOS of region 1 and region 2. The numerator of η means the overlap area between region 1 and region 2. The denominator of η is the normalized VDOS area of a region. A small value of overlap factor η indicates a poor overlap between the two spectra possess, a big overlap factor η means a small mismatch between two regions.

3. Results and discussion

In this paper, thermal conductivity of a monolayer graphene sheet with a length of 24.5 nm and a width of 2.46 nm was calculated. By assuming the thickness of the graphene sheet as 1.42 Å, the thermal conductivity was calculated to be 247.5 ± 17.7 W·m^{-1}·K^{-1}. The size of the graphene sheet in our work is close to that of the Ref. [30] (a graphene sheet with a size of 29 nm×5.8 nm×0.142 nm). Our result was in good agreement with the reported value of ~230 W·m^{-1}·K^{-1}.[30] The obtained result confirmed the validity of the simulation method used here. Before investigating thermal transport in the 3D hybrid structures, the thermal conductivity of overlapped graphene sheets without junctions was calculated, and the result was 6.27 ± 0.05 W·m^{-1}·K^{-1}.

3.1. Influence of CNR diameter on the thermal conductivity

In reality, the position of CNR linkers may be random. Thus, it is necessary to examine the influence of location of the linkers. Typical CNR linker locations are shown in Fig. 2, and thermal conductivities of CNR–graphene structures are provided in Table 1.

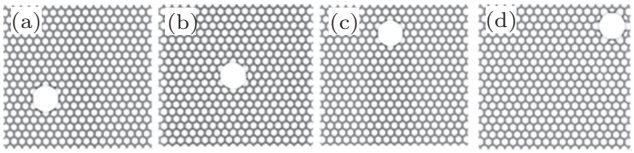


Fig. 2. Position of CNR linkers. (a)–(c) CNR is located in non-edge region; (d) CNR linker located in edge region.

Table 1. Thermal conductivities of CGHS with different linker position.

CNR linker position	Fig. 2(a)	Fig. 2(b)	Fig. 2(c)	Fig. 2(d)
Thermal conductivity/W·m^{-1}·K^{-1}	58.5±5.7	60.1±2.1	59.5±4.3	40.7±3.2

If a CNR linker locates in the marginal area (Fig. 2(d)), thermal conductivity of CNR–graphene structure is around 40 W·m^{-1}·K^{-1}. While a CNR is located in non-edge region (Figs. 2(a)–2(c)), the thermal conductivity is increased to 60 W·m^{-1}·K^{-1}. The state of stress is expected to alter the wave speeds as well as phonon dispersion relations in graphene.[31] When the CNR linker is located in marginal area, the structure of graphene is distorted significantly and the conjugated structure is destroyed, increasing the scattering of phonons. This result showed that linker location hardly affects the thermal conductivity of CGHS except for marginal area.

Hence, in the following, we only focus on the cases with CNR linkers in center region.

To investigate the influence of CNR diameters on the thermal conductivities, the diameters of CNRs were varied from 0.407 nm to 2.441 nm. The geometrical parameters of the CNRs are shown in Table 2.

Table 2. Various diameters of CNRs in simulation.

CNR type	Width of graphene sheets/nm	Diameter of CNRs/nm	λ^{a}
(3,3)	4.26	0.407	0.9
(6,6)	4.26	0.814	0.81
(9,9)	4.26	1.22	0.72
(12,12)	4.26	1.627	0.62
(15,15)	4.26	2.034	0.52
(18,18)	4.26	2.441	0.43

Note: [a] Ratio of effective width /graphene sheet width.

As shown in Fig. 3, the thermal conductivities increase at first and reaches a peak value, then, take a downtrend, with growth of the diameter. Early studies explained that there are more phonon branches in a CNT with larger diameter.[32,33] Those reports imply that more phonons are available to contribute to heat transfer in a bigger CNR. Furthermore, larger diameter also brings larger contact area at the interface, i.e., there would be more covalent bonds formed at the interface. Therefore, with increased diameters, more heat is transported across CNR–graphene junctions. As the diameters increase to 1.22 nm, the thermal conductivities approach a peak value of 65 $W{\cdot}m^{-1}{\cdot}K^{-1}$.

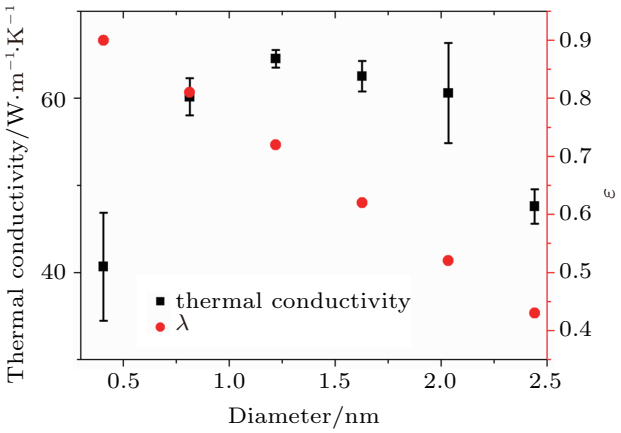


Fig. 3. (color online) Thermal conductivities of CGHS versus the diameter of linkers.

However, with the diameters of CNR increased to 2 nm, the thermal conductivities drop sharply. This phenomenon is attributed to the ballistic nature of thermal transport. The structure of graphene is seriously damaged, for the ratio of $EW/W(\lambda)$ is approximately 0.52 (as shown in Table 2). Hence, although the CNR–graphene junctions enhanced the interfacial thermal transport, the thermal transport within the graphene sheet was severely obstructed by CNRs.[34–36] As for $\lambda > 0.4$, the thermal conductivities are significantly reduced by the decreasing of λ.[37]

In this case we note that both diameters and λ affect overall thermal transport in CGHS. The in-plane thermal conductivity is expected to be affected by phonon scattering at the CNR–graphene junctions on the graphene sheets in each unit cell. On the basis of above discussion, it is evident that both CNR diameters and λ are key factors in governing thermal transport in graphene sheets and across two graphene sheets.

3.2. Influence of CNR number on the thermal conductivity

The number of (6, 6) CNR with height of 0.246 nm was selected to study effects of CNRs number on thermal conductivity of CGHS. In order to reduce arrangement impact on thermal conductivity, all CNR linkers were transversely aligned as shown in Fig. 4.

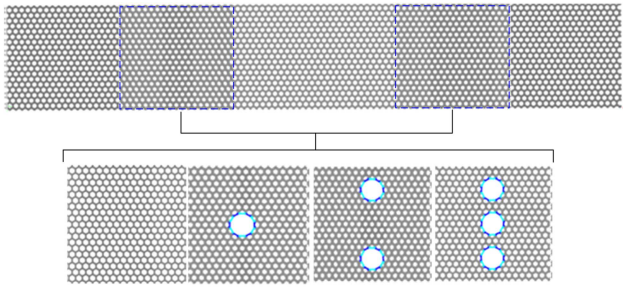


Fig. 4. (color online) Schematic diagram of CNR arrangements on graphene sheets.

As it can be seen in Fig. 5, the thermal conductivities increase at beginning and drop gradually when CNR linker number > 2. By bridging the graphene sheets with two linkers, the thermal conductivities increase to 68.8 $W{\cdot}m^{-1}{\cdot}K^{-1}$.

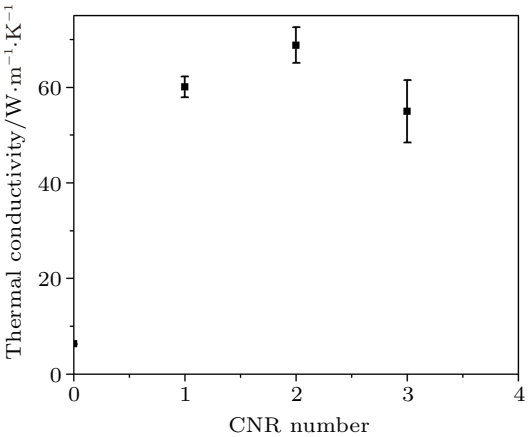


Fig. 5. Thermal conductivities of CGHS versus CNR number.

Such a phenomenon could be understood from the following reasons. When the linkers are sparse, the junctions retard the in-plane thermal conduct mildly, and more heat could conduct from CNR–graphene junctions with increasing linkers. However, when the linkers are much denser, graphene sheets are divided into small pieces. This will reduce in-plane phonon transmission channels, leading to lower thermal conductivity. In addition, the bond length in a hexagonal carbon

ring of graphene is 0.142 nm while the bond length in a distorted hexagonal carbon ring from the CNR–graphene junction region is in the range 0.138 nm∼0.143 nm. This confirms that the hexagonal carbon rings in CNR–graphene junctions have been seriously twisted.

We further analyzed the distribution of VDOS under different region. Figure 6 shows the VDOS in a region of normal hexagonal carbon rings and a region of distorted hexagonal carbon rings. The two kinds of VDOS are alike on the whole. However, the peaks of the VDOS hardly match in both high frequency and low frequency regions. η of pristine graphene and distorted graphene is 0.404. So the distorted hexagonal carbon rings are expected to play the role of defects in graphene giving rise to phonon scattering and producing a thermal resistance at the CNR–graphene junctions.

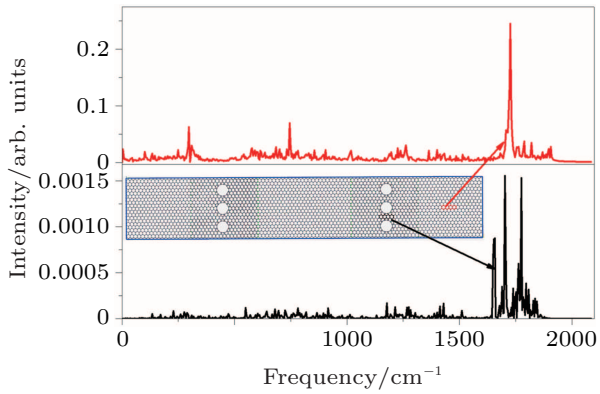


Fig. 6. (color online) VDOS of graphene in the selected regions.

Thermal resistance of the CGHS with 3 linkers in a row is dominated by the thermal conduction in a single graphene sheet. If linker number > 2, the reduction of the cross-plane thermal resistances are relatively small in comparison with growth of the in-plane thermal resistances with increasing of linkers.

These results agree well with the findings of arshney *et al.*[38] and Jungkyu Park *et al.*[27] Vikas Varshney *et al.* and Jungkyu Park *et al.* analyzed thermal transport in three-dimensional CNT–graphene superstructures and found that out-of-plane thermal conductivities decreased and in-plane thermal conductivities increased near linearly with decreasing CNT numbers. With linker number increasing, phonon transmission tunnels also increase, leading to smaller interlayer thermal resistance. However, high density linkers decrease the overall phonon mean-free-path, leading to lower in-plane thermal conductivities. Therefore, a reasonable CNR density is essential for a high thermal conductivity structure.

3.3. Influence of CNR height on the thermal conductivity

The shortest CNR with height of 0.246 (CNR-0.246) and reference CNRs with height of 0.492 nm (CNR-0.492) and 0.738 nm (CNR-0.738) were selected to identify height influence on thermal conductivity. Comparing CNR-0.492 and CNR-0.738 to CNR-0.246, the thermal conductivities of CGHSs decreased by 6% and 7%, respectively. This can be explained by the special structure of CNR-0.246. As shown in Fig. 7, there is no bulk region in the CNR-0.246, while there is a CNR bulk region in the higher CNR linker. Since the crystal structures at interface and central regions are quite different, phonons scatter at junction boundaries, which lead to a low thermal conductivity.

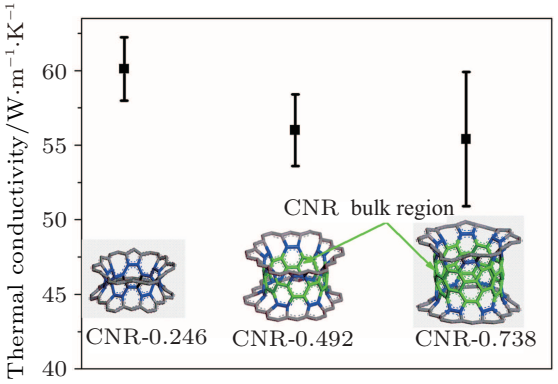


Fig. 7. (color online) Thermal conductivities of CGHS with different linker heights.

To authenticate the above discussion, the VDOS of CNR interface region and CNR bulk region was investigated (Fig. 8). It can be observed that the VDOS distribution is similar. But there is a small overlap between peaks of the two spectra both in the high frequency and low frequency region. The quantity η between CNR interfacial region and CNR bulk region was also calculated, and the result was 0.63, which confirmed the occurrence of phonon scattering between CNR interfacial region and CNR bulk region.

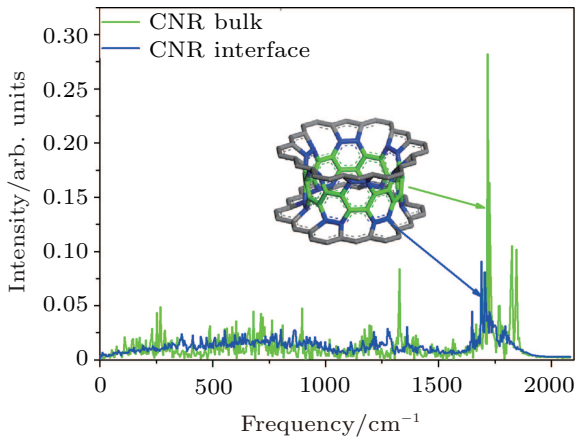


Fig. 8. (color online) VDOS of CNR interface region and CNR bulk region.

4. Conclusion

In summary, MD simulations were conducted to investigate the effects of CNR linkers on the interlayer thermal conduction between two graphene sheets. It is found that

the thermal conductivity of overlapped graphene sheets increases significantly with 2 covalent-bonded CNRs, and tops at 68.8 $W{\cdot}m^{-1}{\cdot}K^{-1}$, 28% of that of single-layer graphene sheet, and 11 times higher than that of overlapped graphene sheets without CNRs.

The diameter of CNR and density of CNR are found to be the two most important parameters which govern the thermal transport in the CNR–graphene hybrid structures. On one hand, bigger CNR linkers or more CNR linkers dictate great phonon scattering at CNR–graphene junctions, which decreased in-plane thermal conductivity of an individual graphene sheet. On the other hand, they increase the phonon transport tunnels from one graphene sheet to another. The shortest CNR could enhance the thermal conductivity of hybrid structure, which can be attributed to avoid phonon scattering between the CNR buck region and CNR interfacial region. Thus, for the development of graphene joints or junctions, the diameter and concentration of cross-linkers should be optimized. Our present work indicates that optimally controlling the number of CNR linkers between graphene sheets can be an effective and practical approach to optimize the thermal conduction across the graphene sheets.

References

[1] Zhang G and Zhang Y W 2017 *Chin. Phys. B* **26** 034401
[2] Subrina S, Kotchetkov D and Balandin A A 2010 12*th IEEE Intersociety Conference on Thermal and Thermomechanical Phenomena in Electronic Systems*, June 2–5, 2010, Las Vegas, USA, p. 5343
[3] Gao Z, Zhang Y, Fu Y, Yuen M and Liu J 2013 *Electronic Components & Technology Conference*, May 28–31, 2013, Las Vegas, USA, p. 2075
[4] Xin G, Sun H, Hu T, Fard H R, Sun X, Koratkar N, Borca-Tasciuc T and Lian J 2014 *Adv. Mater.* **26** 4521
[5] Yu W, Xie H, Li F, Zhao J and Zhang Z 2013 *Appl. Phys. Lett.* **103** 141913
[6] Balandin A A, Ghosh, S, Bao W, Calizo I, Teweldebrhan D, Miao F and Lau C N 2008 *Nano Lett.* **8** 902
[7] Liu X, Zhang G and Zhang Y W 2014 *J. Phys. Chem. C* **118** 12541
[8] Pop E, Varshney V and Roy A K 2012 *MRS Bull.* **37** 1273
[9] Niu J, Li M, Choi W, Dai L and Xia Z 2014 *Carbon* **67** 627
[10] Niu J, Li M and Xi Z 2014 *RSC Adv.* **4** 33848
[11] Yang Z, Zhao Y, Xiao Q, Zhang Y, Jing L, Yan Y and Sun K 2014 *ACS Appl. Mater. Interfaces* **6** 8497
[12] Du F, Yu D, Dai L, Gangul S, Varshne V and Roy A K 2011 *Chem. Mater.* **23** 4810
[13] Zheng Q, Li Z, Yang J and Kim J K 2014 *Prog. Mater. Sci.* **64** 200
[14] Dimitrakakis G K, Tylianakis E and Froudakis G E 2008 *Nano Lett.* **8** 3166
[15] Radoslaw P W and Terzyk A P 2011 *Phys. Chem. Chem. Phys.* **13** 17027
[16] Sun J, Liu H, Chen X, Evans D G, Yang W and Duan X 2013 *Adv. Mater.* **25** 1125
[17] Zhang J, Shi G, Jiang C, Ju S and Jiang D 2015 *Small* **46** 6197
[18] Mullerplathe F 1997 *J. Chem. Phys.* **106** 6082
[19] Zou J H, Ye Z Q and Cao B Y 2016 *J. Chem. Phys.* **145** 134705
[20] Si C, Wang X D, Fan Z, Feng Z H and Cao B Y 2017 *Int. J. Heat Mass Transfer* **107** 450
[21] Sun H 1998 *J. Phys. Chem. B* **102** 7338
[22] Zhang J, Jiang C, Jiang D and Peng H 2014 *Phys. Chem. Chem. Phys.* **16** 4378
[23] Feng Y, Zhu J and Tang D W 2014 *Chin. Phys. B* **23** 083101
[24] YangY L and Lu Y 2014 *Chin. Phys. B* **23** 106501
[25] Xu Z and Buehler M J 2009 *Nanotechnology* **20** 185701
[26] Zhang C, Hao X L,Wang C X, Wei N and Rabczuk T 2017 *Sci. Rep.* **7** 41398
[27] Park J and Prakash V J 2013 *Mater. Res.* **28** 940
[28] Feng D L, Feng Y H, Chen Y, Li W and Zhang X X 2013 *Chin. Phys. B* **22** 016501
[29] Shi J, Dong Y, Fisher T and Ruan X 2015 *J. Appl. Phys.* **118** 044302
[30] Xu L, Wei N, Zheng Y, Fan Z, Wang H Q and Zheng J C 2012 *J. Mater. Chem. A* **22** 1435
[31] Kuang Y, Lindsay L and Huang B 2015 *Nano Lett.* **15** 6121
[32] FengY, Zhu J and Tang D W 2015 *Phys. Lett. A* **379** 382
[33] Yue S, Ouyang T and Hu M 2015 *Sci. Rep.* **5** 15440
[34] Liu D, Yang P, Yuan X, Guo J and Liao N 2015 *Phys. Lett. A* **379** 810
[35] Cao B Y, Yao W J and Ye Z Q 2016 *Carbon* **96** 711
[36] Feng T, Ruan X, Ye Z and Cao B 2015 *Phys. Rev. B* **91** 224301
[37] Yarifard M, Davoodi J and Rafii-Tabar H 2016 *Comput. Mater. Sci.* **111** 247
[38] Varshney V, Patnaik S S, Roy A K, Froudakis G and Farmer B L 2010 *ACS Nano* **4** 1153